Electronic Supplementary Information (ESI)

Large-scale Co_3O_4 nanoparticles growing on nickel sheet *via* one-step strategy and their ultra-highly reversible redox reaction toward supercapacitors

Changzhou Yuan*[a], Long Yang[a], Linrui Hou[a], Laifa Shen[b], Fang Zhang[b], Diankai Li[a], and Xiaogang Zhang*[b]

[a] *Anhui Key Laboratory of Metals and processing, School of Materials Science and Engineering, Anhui University of Technology, Ma`anshan, 243002, P.R. China.*

[b] *College of material Science and Engineering, Nanjing University of Aeronautics and Astronautics, Nanjing, 210016, P.R. China.*

E-mail:ayuancz@163.com; azhangxg@163.com

Experimental

1. Preparation of cobalt oxide NPs growing on the nickel sheets:

All the chemicals used here were of analytical grade. $Co(NO_3)_2 \cdot 6H_2O$, NH_4NO_3 and ammonia (25 wt.%) were obtained from Nanjing Chemical Company (Nanjing, China). All aqueous solutions were freshly prepared by using high-purity water (18 MΩ cm resistance) from an Ampeon 1810-B system (Jiangsu, China). Nickel sheet substrate was degreased with acetone, etched with 2 M HNO_3 for 10 min and rinsed with water extensively. The edges of the nickel sheet are 0.15 mm in width. In a typical synthesis, $Co(NO_3)_2 \cdot 6H_2O$ (10 mmol) and NH_4NO_3 (5 mmol) were dissolved in a solution consisting of 35 mL H_2O and 18 mL ammonia (25 wt.%). Then, the homogeneous solution and the pretreated nickel sheet were transferred into a Teflon-lined stainless steel autoclave. The autoclave was sealed and maintained at 90 °C for 14 h. After cooled to room temperature, the nickel sheet coated with black samples were rinsed under ultrasonication, and dried at 80 °C for 12 h. In average, 0.51 mg Co_3O_4 NPs were grown on the 1 cm^2 nickel sheet.

Sample characterization:

The samples were examined by powder X-ray diffraction (XRD) (Max 18 XCE, Japan) using

a Cu K_a source (λ = 0.1542 nm) at a scanning speed of 3°/min over a 2θ range of 10° ~ 80°. Scanning electron microscopy (SEM) images and energy dispersive analysis by X-ray (EDAX) were taken with a field-emission scanning electron microscope (FESEM, JEOL-6300F, 15 kV). Microscope, EDAX and selected area electron diffraction (SAED) were performed with transmission electron microscope (TEM, FEI, TECNAI-20) coupled with an energy dispersive X-ray analyzer (Link-200, Britain). X-ray photoelectron (XPS) measurements were performed on a VGESCALAB MKII X-ray photoelectron spectrometer with an Mg_{ka} excitation sources (1253.6 eV).

3. Electrochemical experiments:

The nickel sheet (1 cm^2) supported Co_3O_4 NPs acted as working electrode for following electrochemical tests by cyclic voltammetry (CV) and chronopotentiometry (CP) performed with a CHI660C electrochemical workstation. All experiments were carried out in a three compartment cell with a working electrode, a platinum plate counter electrode and a saturated calomel electrode (SCE) reference electrode at room temperature. The electrolyte was 2 M KOH aqueous solution.

The SCs of the Co_3O_4 NPs growing on nickel sheet were calculated from the CP curves based on the following equation:

$$C = \frac{It}{\Delta V}$$

where C, I, t and ΔV are the SC (F g^{-1}) of the Co_3O_4 NPs growing on nickel sheet electrode, the discharging current density (A g^{-1}), the discharging time (s) and the discharging potential range (V), respectively.

An important parameter, columbic efficiency (η) of the electrode, can be evaluated from the following equation based on the CP plots depicted in Fig. 3c:

$$\eta = \frac{t_D}{t_C} \times 100\% \qquad (2)$$

where t_D and t_C are the time for galvanostatic discharging and charging, respectively.

Sample Characterizations

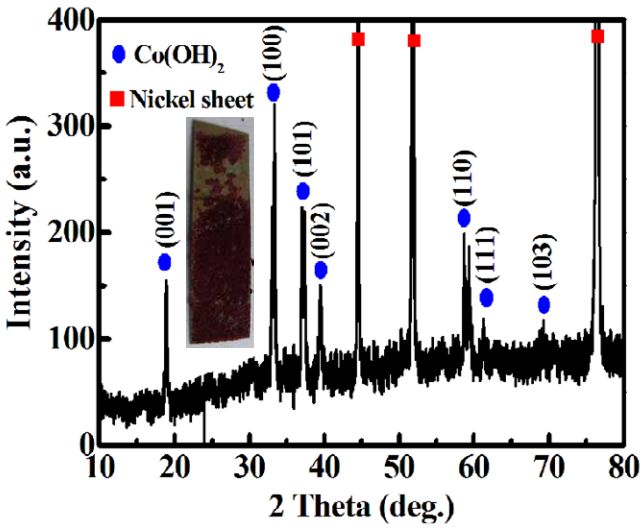

Fig. S1 XRD pattern and digital image (the inset) of the $Co(OH)_2$ sample growing on the nickel sheet pretreated by HCl.

The color of pink indicates the formed phase should be $Co(OH)_2$, rather than Co_3O_4. In addition, all of the reflection peaks for the sample can be indexed as β-$Co(OH)_2$ (Joint Committee on Powder Diffraction Standards (JCPDS), Card No. 30-0443) except three peaks of the nickel sheet as indicated. Moreover, it can be found that the $Co(OH)_2$ cannot be deposited uniformly upon the nickel sheets pretreated by HCl. Moreover, just after the sonication lasting for 5 minutes, all the $Co(OH)_2$ was separated from the nickel substrate, indicating the weak adhesion to the nickel sheet.

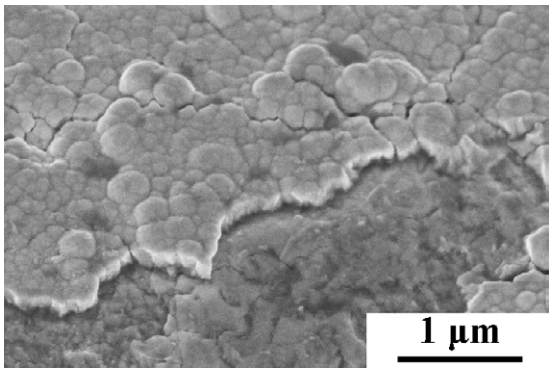

Fig. S2 FESEM image of the Co_3O_4 NPs growing on nickel sheets after sonication for 8 h

As demonstrated in Fig. S2, the Co_3O_4 NPs also can keep strong adhesion to the nickel sheet etched by HNO_3 except some exfoliation of NPs from the nickel sheet substrate even after sonication for 8 h. And from the cross section, the thickness of the Co_3O_4 NPs layer is *ca.* 160 nm.

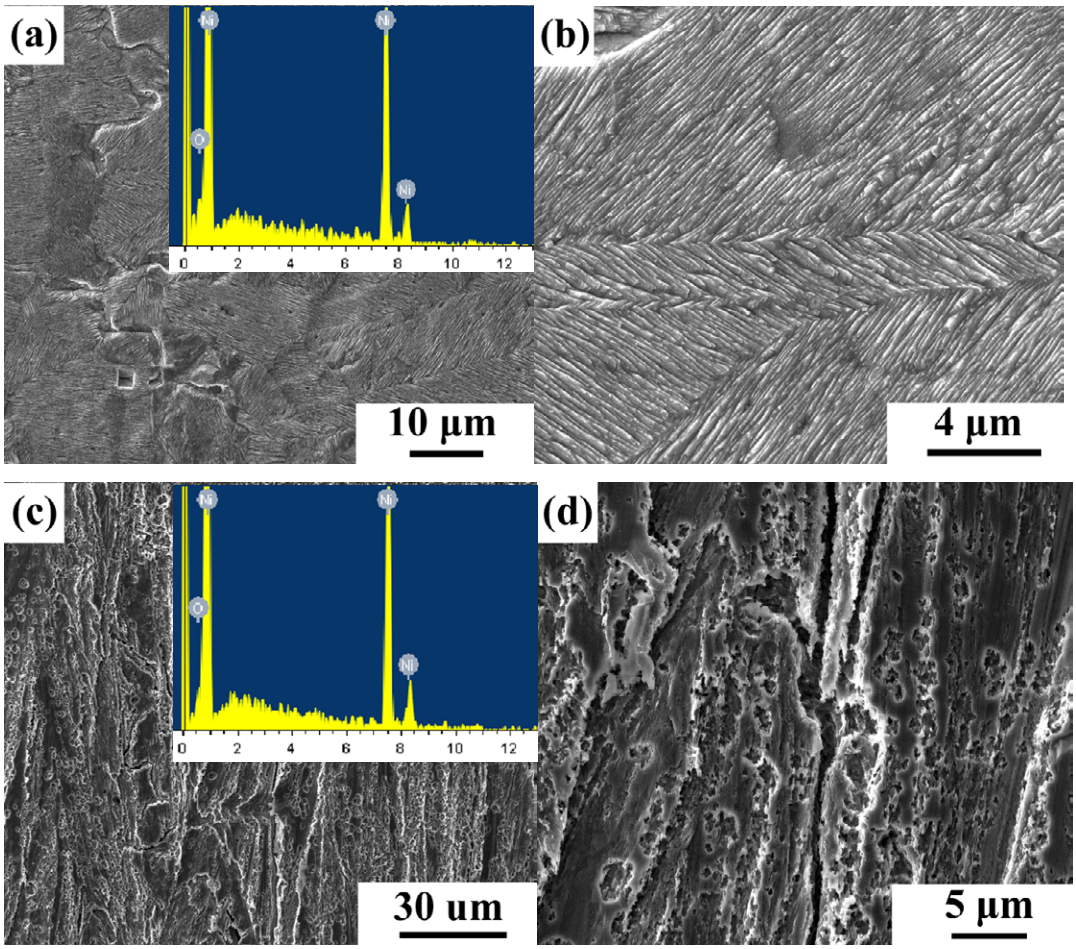

Fig. S3 FESEM images and EDAX data of the nickel sheets etched by (a, b) HNO_3 and (c, d) HCl, respectively.

Clearly, the surface morphologies of the nickel sheets etched by HNO_3 and HCl present different microstructures, as shown in Fig. S3. After etched by HNO_3, the nickel sheet presents a relative smooth surface (Fig. S3a and b). In sharp contrast, the surface of nickel sheet turns out to be much coarse (Fig. S3c and d) after etched by HCl. More importantly, the oxygen content of the two surfaces great differs from each other. For the surface of the nickel sheet etched by HNO_3, the atomic ratio of O and Ni is *ca.* 5 : 95, which is much higher than that of 0.6 : 99.4 for the surface of the nickel sheet etched by HCl, according to the EDAX data in the insets.

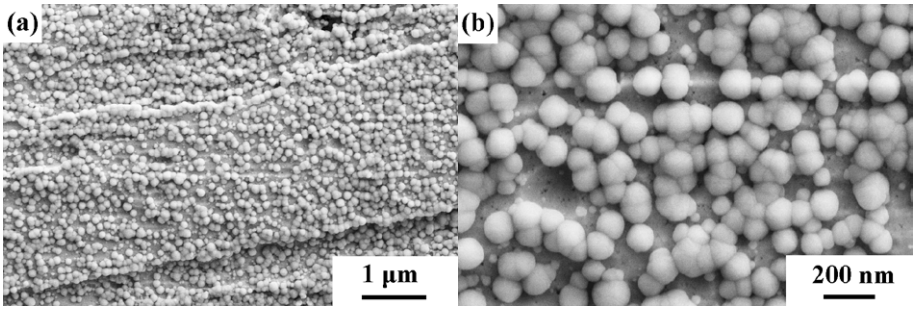

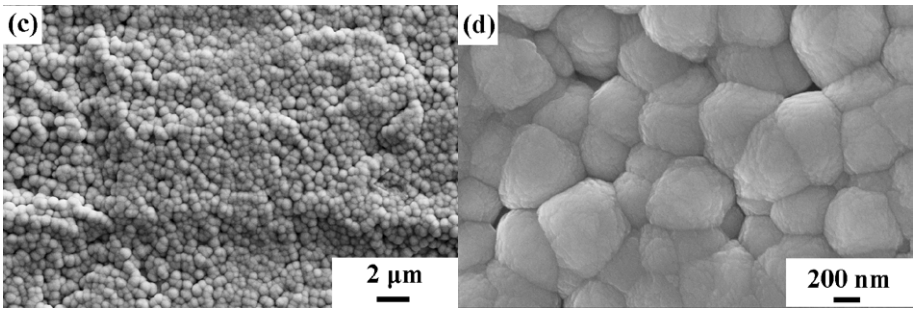

Fig. S4 FESEM images of the Co_3O_4 NPs obtained by hydrothermal treatment for different time. (a, b) 7 h; (c, d) 28 h.

As seen from FESEM images (Fig. S4a and b) of the Co_3O_4 NPs growing on the surface of the nickel sheet after hydrothermal treatment for 7 h, lots of Co_3O_4 NPs with the size of *ca.* 100 nm scatteredly dispersed on the surface of the nickel sheet. And the loading of the Co_3O_4 is *ca.* 0.21 mg cm^{-2} for such case. While after 28 h, the Co_3O_4 NPs compactly dispersed upon the nickel sheet with the loading of *ca.* 0.95 mg cm^{-2} (Fig. S4a). The loadings of Co_3O_4 obtained after different hydrothermal time are all lower than other reports. [1-3] The lower loading of Co_3O_4 NPs would facilitate the electrolyte ions to contact the rich electroactive surface of Co_3O_4 NPs for energy storage. Thus, much better electrochemical performance can be delivered than others. [1-3] Of note, the size of CO_3O_4 NPs increases up to *ca.* 400 nm after the longer hydrothermal treatment for 28h, which is much larger than that of CO_3O_4 NPs obtained after hydrothermal treatment for 7 h and 14 h. Therefore, it is easily concluded that the loadings of Co_3O_4 NPs can be adjusted by changing the hydrothermal time. The longer time for hydrothermal treatment, the more loadings of Co_3O_4 NPs. Unfortunately, it is difficultly realized to increase the loadings of Co_3O_4 NPs but not increase the size of NPs at the same time.

1. G.L. Wang, D.X. Cao, C.L. Yin, Y.Y. Gao, J.L. Yin and L. Chen, *Chem. Mater.,* 2009, **21**, 5112.

2. Y.Y. Gao, S.L. Chen, D.X. Cao, G.L. Wang and J.L. Yin, *J. Power Sources*, 2010, 1**95**, 1757.

3. X.H. Xia, J.P. Tu, Y.J. Mai, X.L. Wang, C.D. Gu, X.B. Zhao, *J. Mater. Chem.*, 2012, **21**, 9319.

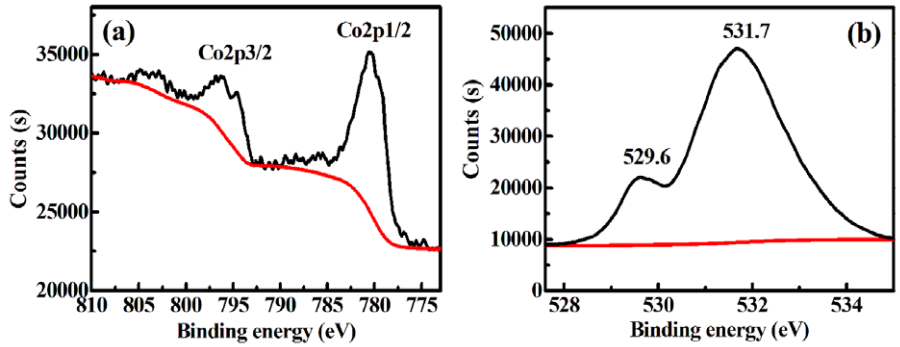

Fig. S5 High-resolution XPS measurements for the Co2p (a) and O1s (b) for the Co_3O_4 NPs growing on the nickel sheet.

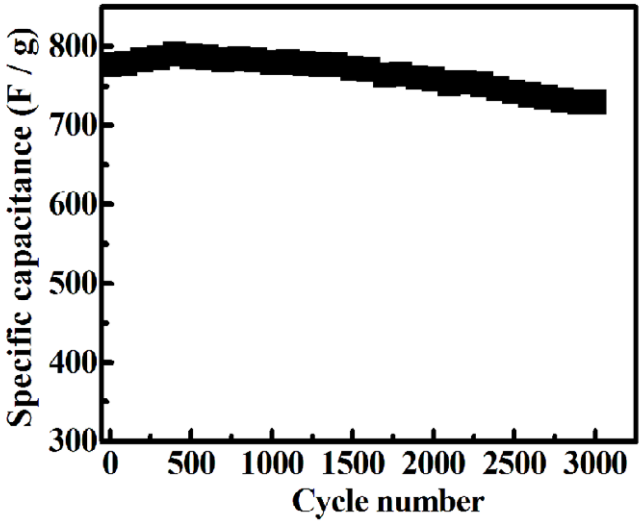

Fig. S6 Cycling performance of Co_3O_4 NPs growing on the nickel sheet at a current of 12 A g^{-1}.